A Combined Simulation and Kirkwood−Buff Approach to Quantify Cosolvent Effects on the Conformational Preferences of Peptides in Solution

Mahalaxmi Aburi[†] and Paul E. Smith*[,‡]

Department of Biochemistry, Kansas State University, Manhattan, Kansas 66506-3702, and Department of Chemistry, Kansas State University, Manhattan, Kansas 66506-3701

Received: August 29, 2003; In Final Form: March 8, 2004

A molecular dynamics study of the effects of salt on the conformational preferences of leucine enkephalin (LE) in water has been performed to outline a general approach for quantifying the effects of a cosolvent on a biomolecular equilibrium in solution using molecular simulation. The simulations of LE suggest that the peptide exists as a mixture of folded and unfolded conformations in pure water, and a potential of mean force calculation indicates the population of the folded form to be 53±3%. The addition of 2 M salt reduces the population of the folded form to 12±5%. A combination of the simulation data and Kirkwood−Buff theory is used to determine the preferential interactions of the cosolvent with the peptide and to reproduce the population changes indicated by the potential of mean force calculations. The results demonstrate the potential of a combined simulation and Kirkwood−Buff approach for quantifying simulation data in an effort to understand the effects of cosolvents on the thermodynamics of biomolecules in solution, especially for systems where potential of mean force calculations are unfeasible.

Introduction

Temperature,[1,2] pressure,[3] pH,[4] and the presence of additives (cosolvents)[5,6] are known to influence the structure and thermodynamic stability of peptides and proteins in solution. Of these, the interaction of cosolvents with peptides and proteins at the atomic level is arguably the least understood. There have been many experimental studies concerning the effects of cosolvents on peptides, proteins, and small molecule models of biochemical interest.[5,7,8] Cosolvents can either increase the solubility of a protein (salting-in effect) or lead to precipitation (salting-out effect). They can also help to stabilize or destabilize secondary structural elements and are commonly used to denature proteins.[9,10] In a three-component system involving a peptide or protein, water, and cosolvent, a knowledge of the preferential interaction (or association) between the protein and each solvent component can be used to rationalize the corresponding cosolvent effects.[11,12] In general, the addition of a cosolvent to a solution will shift the conformational equilibrium in favor of the conformation with the larger preferential interaction with the cosolvent.

Unfortunately, current experimental techniques do not provide atomic detail concerning the relevant binding sites or the degree of binding of cosolvents to proteins. Furthermore, analysis of the thermodynamics of denaturation provides estimated total numbers of bound cosolvent molecules that can vary widely depending on the binding model used for the analysis.[13−15] In principle, computer simulations of peptides or proteins in different solvent environments can provide atomic level detail of the interactions between cosolvent molecules and proteins. However, most previous studies have provided only qualitative descriptions of the effects of different cosolvents[16−22] and do not relate the observations to thermodynamic changes. Here, we describe how quantitative thermodynamic information can be obtained from molecular dynamics (MD) simulations, which can then be used to compare directly with the experimental thermodynamic data and therefore provide insights into the action of different cosolvents. It is not the intent of this study to explain experimentally observed salt effects in general. Rather, an attempt is made to establish a procedure by which they may be studied in a meaningful way using molecular simulation.

The effects of 2 M NaCl on a small model peptide were examined by using computer simulation data to determine the preferential interactions of NaCl with the peptide. The corresponding thermodynamic changes were then evaluated using Kirkwood−Buff (KB) theory.[23,24] A high salt concentration (2 M) was used to provide good statistics for a full analysis of the salt effects, while a small peptide was chosen so that the effects of salt could be quantified by more than one method; thereby eliminating the inaccuracies in the force field parameters. The model peptide used in this study was leucine enkephalin (LE), an endogenous opioid pentapeptide (YGGFL) with morphine-like activity.[25] In a previous simulation study of LE in pure water the peptide was observed to fluctuate between folded and unfolded forms, thus providing a simple model of a reversible process.[26] The peptide also displays the major features associated with larger proteins, i.e., the presence of charged groups (N and C termini), a polar peptide backbone, and hydrophobic side chains (Tyr, Phe, and Leu).

Although the effect of salt on LE is unknown, the peptide provides a model for a conformational equilibrium which is accessible by simulation. Experimentally, it is known that NaCl salts-in the peptide group and salts-out hydrophobic groups.[7,27−29] The corresponding effect on charged residues is unknown but there is potential for ion pairing (between the termini and ions) and for screening of the interactions between the terminal groups. The presence of many different groups within the peptide makes the effect of salt on the equilibrium difficult to

* Corresponding author. Paul E. Smith, Department of Chemistry, 111 Willard Hall, Kansas State University, Manhattan, KS 66506-3701, Fax: 785-532-6666, E-mail: pesmith@ksu.edu.

[†] Department of Biochemistry.

[‡] Department of Chemistry.

10.1021/jp036582z CCC: $27.50
Published on Web 04/30/2004

TABLE 1: Summary of the MD Simulations[a]

simulation	N_s	N_c	N_w	V (nm^3)	T_{sim} (ns)
H_2O			1015	31.28	2
2M NaCl		68	947	30.06	2
LE/H_2O	1		1015	31.89	25
LE/2M NaCl	1	68	947	30.74	20

[a] Symbols: N_s, the number peptide solutes; N_c ($= N_+ + N_-$), the total number of indistinguishable ions; N_w, the number of water molecules; V, the average volume of the system; and T_{sim}, the total simulation time.

predict. Using a combination of simulation data and KB theory, a quantitative description of the effect of salt on this equilibrium is obtained. In addition, a determination of the contributions from individual groups and residues toward the total preferential interaction is attempted.

Methods

All molecular dynamics simulations were performed using the GROMOS96 program and the 43a1 force field.[30] The SPC water model[31] and a truncated octahedron were used for the simulations. The time-step was 2 fs and SHAKE[32] was used to constrain all bond lengths with a tolerance of 10^{-4} nm. A twin range cutoff of 0.8 nm/1.4 nm was employed and the nonbonded pair list was updated every 10 steps. Long-range electrostatics were treated using the Poisson−Boltzmann reaction field approach,[33] with a reaction field permittivity for SPC water of 54.[34] This treatment of electrostatic interactions has been shown to be free from major cutoff artifacts and to provide results comparable to the Ewald technique.[33] The simulations were performed under conditions of constant temperature (300 K) and constant pressure (1 atm) using the weak coupling approach.[35] The simulation of LE in pure water has been described previously.[26] The initial configuration for the simulation in saline solution was obtained by randomly replacing water molecules with ions to achieve the desired ratio of ions to water, which resulted in a final salt concentration of 1.88 M. The system was then minimized using 100 steps of steepest descent and simulated for 20 ns. Configurations were saved every 1 ps for analysis. A summary of the simulations is presented in Table 1.

The potential of mean force (pmf) between the N_2 and C_5 atoms was determined in pure water and in saline solution using umbrella sampling[36] with a harmonic distance restraining potential and a force constant of 10,000 kJ/mol/nm^2. A series of runs was performed differing only in the position of the reference distance, which varied from 0.30 to 1.25 nm in increments of 0.05 nm. Probability distributions corresponding to the N_2 to C_5 distance were then obtained from 1 ns and 3 ns of simulation performed in each window for the pure water and saline solution pmfs, respectively. Configurations were saved every 0.05 ps. After correcting the data for the presence of the biasing function, the resulting set of histograms were then combined to generate the final pmf using the WHAM approach.[37] Throughout this work the folded form is defined as any conformation with an N_2 to C_5 distance less than 0.5 nm.

A cluster analysis was performed using previously described methods.[38,39] Clustering was performed based on comparisons of the backbone root-mean-square deviation (rmsd) of the N, C^α, C, and O atoms. A rmsd value of 0.1 nm was used to distinguish the clusters. In addition to clustering the pure water and saline solution trajectories individually, the trajectories from both simulations have been combined and clustered in an attempt to highlight similarities and differences between conformations sampled in the absence and presence of salt.

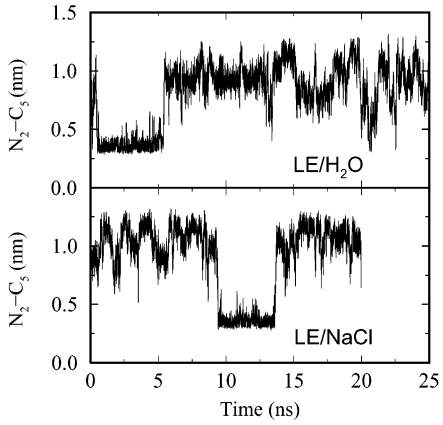

Figure 1. Time histories for the N_2-C_5 distance obtained from the simulations in pure water and 2 M saline solution. This distance was used to define folded (<0.5 nm) and unfolded (> 0.5 nm) conformations.

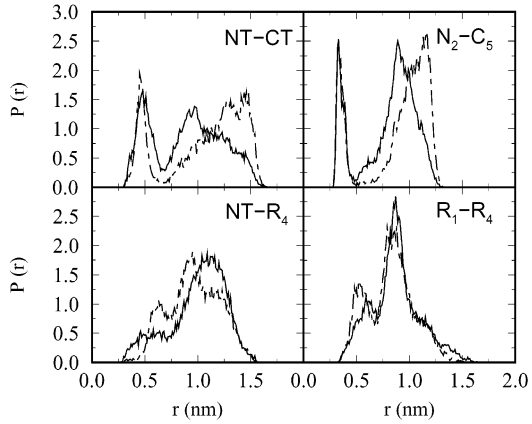

Figure 2. Probability distribution between different groups of LE obtained from the simulations in pure water (solid line) and 2 M saline solution (dashed line). R1 and R4 denote the aromatic rings of Tyr and Phe, using the center of mass to define the ring positions.

Results

The time histories of the N_2 to C_5 distance for LE in pure water and 2 M NaCl are displayed in Figure 1. The time histories illustrate the formation of a stable folded conformation in both water and NaCl solutions after 1 ns and 9 ns, respectively. The details of the folded structure formed in pure water have been described previously.[26] The same folded turn structure possessing an average N_2-C_5 distance of 0.36 nm occurred in both simulations. Some of the effects of salt on the structure of the peptide are illustrated in Figures 2 and 3. Figure 2 displays the distance probability distributions between different groups within the peptide. The effect of salt on the folded conformation appeared to be relatively minor with both simulations displaying high populations at an NT−CT distance of 0.50 nm and an N_2-C_5 distance of 0.36 nm. However, the nature of the unfolded state was perturbed such that larger NT−CT distances were observed, suggesting a decreased interaction between the charged termini.

The degree of binding of ions to both the folded and unfolded conformations is illustrated in Figure 3 using radial distribution functions (rdfs) obtained from the simulation in saline solution. Both sodium and chloride ions interacted more strongly with the unfolded state. The distribution of sodium and chloride ions around the corresponding charged termini increased on unfolding. However, the increased degree of interaction was not just a consequence of direct binding to the peptide but involved

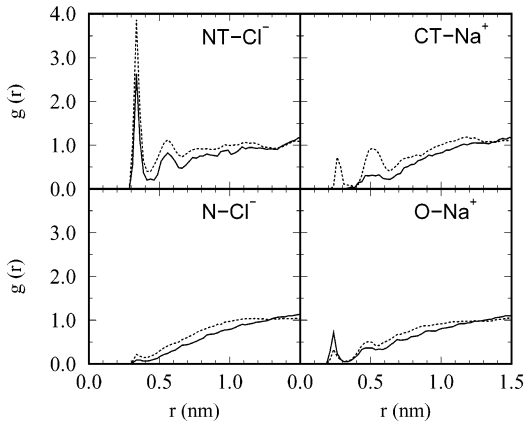

Figure 3. Radial distribution functions obtained for the folded (solid line) and the unfolded (dashed line) conformations in 2 M saline solution. See Table 2 for definitions.

TABLE 2: Coordination Numbers Obtained for LE in 2M NaCl[a]

pairs	R_m (nm)	CN_F	CN_U
NT−Cl^-	0.42	0.20	0.32
CT−Na^+	0.34	0.00	0.05
O−Na^+	0.31	0.03	0.02
N−Cl^-	0.41	0.01	0.03

[a] Coordination numbers of sodium and chloride ions to atoms of LE for the folded and unfolded conformations (CN_F and CN_U) obtained by integration to the first minimum, R_m of the corresponding rdfs. NT and CT correspond to the terminal N and C atoms, O represents an average over the backbone carbonyl oxygen atoms, and N represents an average over the backbone nitrogen atoms.

changes in the ion distributions over a range of distances (0.5 nm or more) away from the peptide surface. This was also illustrated by the first shell coordination numbers presented in Table 2. The small differences observed between the folded and unfolded conformations indicated that the effects of salt arose primarily from changes in the degree of association (extending over many solvation shells) rather than from changes in direct binding to the peptide within the first solvation shell. This situation is characteristic of a weak binding system in which there are no specific long residence time binding sites.

As a further comparison of the peptide conformations observed in pure water and saline solution a clustering analysis was performed on the trajectories using conformations from both simulations. By cross clustering the trajectories one can determine to what extent the ensemble of structures obtained in pure water resemble or differ from the ensemble observed in salt solution. The results are presented in Table 3 with representative structures from the top four clusters displayed in Figure 4. Similar conformations were observed in both simulations but, with the exception of the folded conformation (cluster 1), the major clusters typically indicated a preference for either water or saline solution. Of course, the free energy differences presented in Table 3 are approximate (due to sampling limitations), but they do provide an indication as to the changes in relative populations on the addition of salt. Clearly, the effect of salt varied with conformation, especially for the unfolded ensemble, but the majority of conformations favored in saline solution also displayed a significant population in pure water.

The solvent accessible surface areas of the unfolded and folded conformations are presented in Tables 4 and 5. A small increase in the average surface area on unfolding was observed for all residues and groups in saline solution compared to pure

TABLE 3: Clustering Analysis of the Conformations Generated in Pure Water and 2 M NaCl[a]

cluster	population	f^{H_2O}	ΔG^{H_2O} (kJ/mol)	f^{NaCl}	ΔG^{NaCl} (kJ/mol)
1	0.18	0.45	0.4	0.55	0.0
2	0.13	0.75	0.0	0.25	2.6
3	0.07	0.10	6.8	0.90	1.2
4	0.05	0.94	1.7	0.06	5.8
5	0.04	0.56	3.6	0.44	4.2

[a] The results were obtained by clustering 1000 configurations from each of the pure water and saline solution simulations. The values of f^{H_2O} and f^{NaCl} correspond to the fraction of each cluster number which originated from the pure water and saline trajectories, respectively. The approximate (±1 kJ/mol) values of ΔG^{H_2O} and ΔG^{NaCl} indicate the relative free energies of that a particular cluster obtained from the free pure water and saline solution trajectories, respectively, when they were clustered separately. Cluster number 1 corresponds to the folded conformation of LE, while cluster number 2 represents the most populated unfolded conformation.

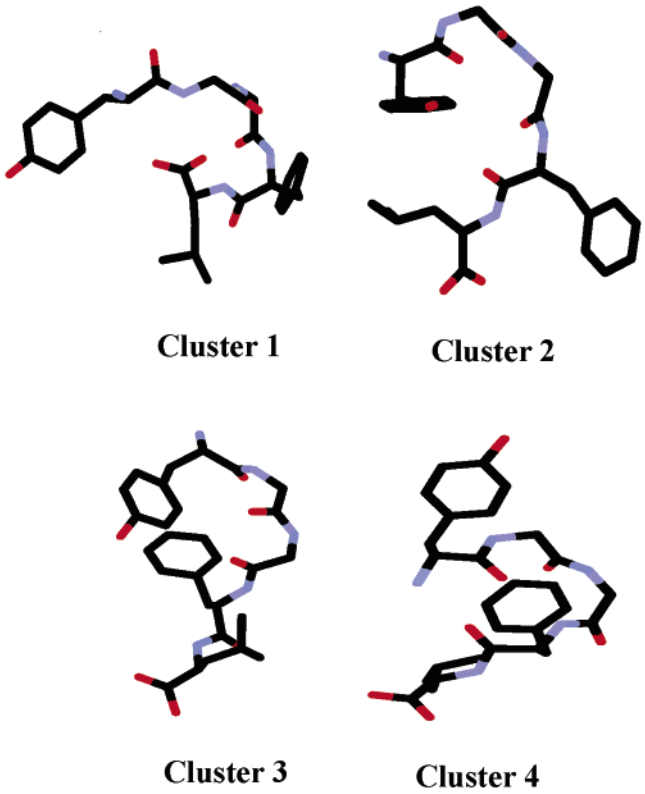

Figure 4. Top four clusters corresponding to the results presented in Table 3. Cluster 1 corresponds to the folded conformation, while clusters 2, 3, and 4 correspond to the three most highly populated unfolded conformations.

water. The surface area of the folded conformation was reduced in the presence of salt, while the average over the unfolded conformations was increased. Analysis of the contributions to the total surface area indicated that the major changes occurred for the Leu residue and the charged groups. This was in agreement with a transition from a folded to unfolded conformation which resulted in exposure of the C terminal (Leu) carboxylate group.[26]

The simulations described here resulted in a population for the folded conformation of 21% and 25% in water and saline solution, respectively. However, the simulations were clearly too short to obtain reliable populations of the folded and unfolded forms due to the relatively few transitions observed (see Figure 1). To obtain more precise populations, the potential of mean force (pmf) between the N_2 and C_5 atoms of LE was

TABLE 4: Residue-Based Accessible Surface Area Changes for LE[a]

	Tyr	Gly	Phe	Leu	Total
LE/H_2O					
F	2.26	1.36	1.85	1.72	7.19
U	2.22	1.32	1.83	2.13	7.50
ΔASA	−0.04	−0.04	−0.02	0.41	0.31
LE/2M NaCl					
F	2.21	1.23	1.78	1.67	6.89
U	2.31	1.28	1.81	2.22	7.62
ΔASA	0.10	0.05	0.03	0.55	0.73

[a] Average residue based solvent accessible surface areas (nm^2) as a function of conformation (F or U) obtained using a probe radius of 0.14 nm and the method of Lee and Richards.[55] The peptide atom radii were taken from the GROMOS force field ($0.5\sigma_{ii}$).

TABLE 5: Group-Based Accessible Surface Area Changes for LE[a]

	charge	polar	nonpolar	total
LE/H_2O				
F	0.78	2.41	4.00	7.19
U	1.26	2.31	3.94	7.51
ΔASA	0.48	−0.10	−0.06	0.32
LE/2M NaCl				
F	0.78	2.22	3.89	6.89
U	1.32	2.32	3.98	7.62
ΔASA	0.54	0.10	0.09	0.73

[a] See Table 4 for details. The charge group included that the N and C^{α} atoms of Tyr together with the C^{α} and CO_2^- atoms of Leu. The polar group included the backbone N, C, and O atoms together with the Tyr C−OH atoms. The nonpolar group included all aliphatic and aromatic ring carbons.

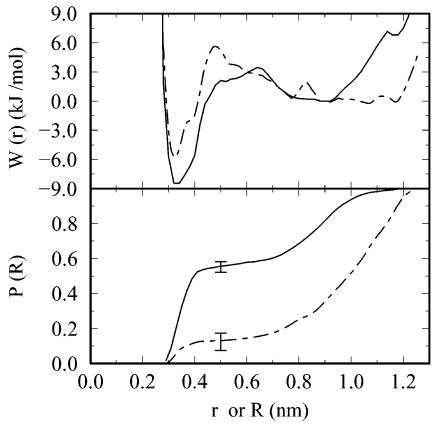

Figure 5. Potential of mean force (top) as a function of distance between the N_2 and C_5 atoms of LE determined in pure water (solid lines) and 2 M saline solution (dashed lines). The corresponding populations (bottom) obtained after integrating the potentials of mean force to a distance *R*.

determined using umbrella sampling techniques. The resulting pmfs in water and 2 M NaCl are presented in Figure 5, together with the corresponding integrated populations. The pmfs resulted in populations for the folded form of 53±3% and 12±5% in pure water and 2 M NaCl, respectively. The decrease in population of the folded state in saline solution suggested that NaCl preferentially associated with the unfolded state over the folded state, in agreement with the data displayed in Figures 2 and 3.

In summary, the GROMOS force field predicts that LE exists in equilibrium between a single folded and several highly populated unfolded forms in both pure water and saline solution. The addition of salt increased the overall population of the unfolded form(s) with an increase in the distance between the charged termini. The change in population was not due to the presence of a single specific binding site but involved a general increase in the degree of ion association with the unfolded peptide occurring over several solvation shells. The system provides a useful example of a salt-dependent equilibrium in a weak binding system.

One of the major difficulties encountered when trying to analyze simulation data on cosolvent effects lies in relating the observed effects to the thermodynamics of the system. Here, Kirkwood−Buff (KB) theory will be used to relate the changes in salt association to the corresponding changes in the conformational populations of the peptide. KB theory has been used extensively for the characterization of binary and ternary liquid mixtures.[40] The theory relates the rdfs between the different solution species to derivatives of the chemical potentials of the components. This is achieved via KB integrals which are defined as[23]

$$G_{ij}(R) = 4\pi\int_0^R [g_{ij}(r) - 1]r^2\,\mathrm{d}r \qquad (1)$$

where $g_{ij}(r)$ is the rdf between species *i* and *j* as a function of center of mass distance *r*. The total chemical potential of a solute (μ_s) in a mixture of cosolvent (c) and water (w) at a constant pressure (p) and temperature (T) can be written as

$$\mu_s(\rho_s,\rho_c,\rho_w,p,T) = \mu_s^{ex}(\rho_s,\rho_c,\rho_w,p,T) + RT\ln(\rho_s\Lambda_s^3 q_s^{-1}) \qquad (2)$$

where *R* is the gas constant, q_s is the solute molecular partition function, Λ_s is the solute thermal de Broglie wavelength, and ρ_i are the corresponding number densities or concentrations. For an infinitely dilute peptide solute, the derivative of the solute excess chemical potential (μ_s^{ex}) with respect to a change in cosolvent number density (ρ_c) is then given by[24]

$$-\beta\left(\frac{\partial\mu_s^{ex}}{\partial\ln\rho_c}\right)_{p,T,\rho_s\to 0} = \frac{\rho_c(G_{sc} - G_{sw})}{1 + \rho_c(G_{cc} - G_{cw})} = \nu_{sc}a_{cc} \qquad (3)$$

where $\beta = 1/(RT)$. The value of a_{cc} is given by

$$a_{cc} = \left(\frac{\partial\ln a_c}{\partial\ln\rho_c}\right)_{p,T} = \frac{1}{[1 + \rho_c(G_{cc} - G_{cw})]} \qquad (4)$$

and is a property of the binary cosolvent solution (in the absence of solute) which varies with composition. The value of ν_{sc} describes the preferential binding of the cosolvent with the solute and indicates the increase in the local cosolvent concentration above that of the bulk solution. This includes both direct binding effects and changes in other, more distant, solvation shells. A positive value for ν_{sc} indicates preferential binding of the cosolvent and leads to a decrease in the solute chemical potential. The preferential binding can also be written as

$$\nu_{sc} = \rho_c(G_{sc} - G_{sw}) = N_{sc} - (\rho_c/\rho_w)N_{sw} \qquad (5)$$

where $N_{ij} = \rho_j G_{ij}$ describes the excess number of *j* species associated with species *i*. For an equilibrium process between a folded and unfolded state characterized by populations (P_i) and an equilibrium constant $K = P_U/P_F = (1-P_F)/P_F$ one has

$$-\beta\left(\frac{\partial(\mu_U^{ex} - \mu_F^{ex})}{\partial\ln\rho_c}\right)_{p,T,\rho_s\to 0} = \left(\frac{\partial\ln K}{\partial\ln\rho_c}\right)_{p,T,\rho_s\to 0} = \Delta\nu_{sc}a_{cc} \qquad (6)$$

where $\Delta\nu_{sc} = \nu^U - \nu^F$ describes the difference in preferential binding of the cosolvent to the folded and unfolded forms. The

TABLE 6: Simulated and Experimental KB Data for a 2 M NaCl Solution[a]

	C_s	ρ	G_{cc}	G_{cw}	G_{ww}	$\bar{V}_c$	$\bar{V}_w$	a_{cc}	ϕ_w
MD	1.88	1.030	204	−24	−16	14.0	18.1	0.54	0.95
exp	1.92	1.072	−42	−8	−17	10.4	18.0	1.15	0.96

[a] Symbols: C_s, salt molarity; ρ, mass density (g/cm^3); and ϕ_w, the water volume fraction. The simulated KB integrals (G_{ij}) and partial molar volumes ($\bar{V}_i$) in cm^3/mol were evaluated assuming $R = 1.0$ nm in eq 1. Experimental data taken from Chitra and Smith.[45]

above equation indicates the direction in which the equilibrium will be perturbed on addition of more cosolvent.

KB theory provides information concerning chemical potential derivatives. Ideally, one should determine the appropriate derivatives at several different cosolvent concentrations and then integrate to obtain the corresponding chemical potential changes. However, this is computationally expensive. Fortunately, many experimentally observed salt effects are known to be proportional to salt concentration,[7,29,41] indicating that the ratio $\partial\mu_s^{ex}/\partial\rho_c = \nu_{sc}\, a_{cc}/\rho_c$ is essentially constant. Therefore, a knowledge of the derivative at one concentration should be sufficient to characterize the changes over the whole concentration range. With this assumption one has

$$\left(\frac{P_U}{P_F}\right)_{\rho_c} = \left(\frac{P_U}{P_F}\right)_{\rho_c=0} e^{\Delta\nu_{sc} a_{cc}} \tag{7}$$

which quantifies the effect of the cosolvent on the relative populations of the folded and unfolded states in terms of the difference in preferential binding ($\Delta\nu_{sc}$), the activity derivative (a_{cc}) of the binary cosolvent solution, and the observed populations in the absence of the cosolvent.

From a simulation of NaCl performed in the absence of the peptide solute, one can obtain the values of G_{ij} and therefore a_{cc} for the cosolvent solution. To do so, the ions have to be treated as indistinguishable to avoid problems associated with electroneutrality.[42−45] Hence, $\rho_c = \rho_+ + \rho_-$ and the value of G_{cc} becomes a composite of the Na−Na, Na−Cl and Cl−Cl rdfs. Furthermore, in the original theory the value of R in eq 1 is set to infinity and the rdfs correspond to the grand canonical ensemble.[23] It has been shown that rdfs obtained from isothermal isobaric simulations can be used if R is taken to be greater than 2−3 solvation shells, but less than half the simulation box length.[46−48] Here, a value of 1.0 nm was adopted as this has been used successful for simple solutes in similar size systems.[48]

The G_{ij} values and the solution properties of 2 M NaCl solution are presented in Table 6 together with the experimental values. The simulations did not reproduce the experimental data very well. In particular, the value of G_{cc} indicated that the simulations displayed too much ion self-association, which resulted in a low value of a_{cc}. Previous studies of the preferential interactions of different urea models suggest that this may lead to values of ν_{sc} that are larger than experimental values.[49] However, even though the agreement with experiment was poor, eq 7 can still be used in an effort to reproduce the population changes obtained from the pmfs, as both sets of data were obtained using the same force field.

The ν_{sc} values obtained from the simulation of LE in 2 M NaCl solution are presented in Tables 7 and 8. Both folded and unfolded conformations displayed exclusion of salt ions from the surface of the peptide, indicating that the peptide solubility would be decreased on addition of salt. The exclusion of salt was larger for the folded form (−4.4±1.0) compared to the unfolded form (−1.8±0.5). Consequently, the value of $\Delta\nu_{sc}$ was

TABLE 7: Residue-Based Preferential Binding Parameters for LE in a 2 M NaCl Solution[a]

		Tyr	Gly	Phe	Leu	Total
F	ν^+	−0.8	−0.3	−0.6	−0.4	−2.1
	ν^-	−0.5	−0.3	−0.9	−0.6	−2.3
	ν^F	−1.3	−0.6	−1.5	−1.0	−4.4 ± 1.0
U	ν^+	−0.3	−0.2	−0.2	−0.3	−0.9
	ν^-	0.4	−0.1	−0.3	−0.9	−0.9
	ν^U	0.1	−0.2	−0.5	−1.2	−1.8 ± 0.5
$\Delta\nu = \nu^U - \nu^F$		1.4	0.4	1.0	−0.2	2.6 ± 1.1
$\Delta\nu/\Delta$ASA		14.0	7.0	35.0	−0.2	55.6

[a] All values were obtained from the simulations assuming $R = 1.0$ nm in eq 1. The preferential binding has been decomposed into contributions from anions and cations ($\nu = \nu^+ + \nu^-$) assuming that $\nu^+ = N_{s+} - (\rho_+/\rho_w)\, N_{sw}$, etc. Changes in accessible surface area (ΔASA) are taken from Table 4.

TABLE 8: Group-Based Preferential Binding Parameters for LE in a 2 M NaCl Solution[a]

		charge	polar	nonpolar	total
F	ν^+	−0.3	−0.5	−1.3	−2.1
	ν^-	0.0	−0.8	−1.5	−2.3
	ν^F	−0.4	−1.3	−2.8	−4.4 ± 1.0
U	ν^+	−0.1	−0.1	−0.8	−0.9
	ν^-	0.1	−0.2	−0.8	−0.9
	ν^U	0.0	−0.3	−1.6	−1.8 ± 0.5
$\Delta\nu = \nu^U - \nu^F$		0.4	1.1	1.2	2.7 ± 1.1
$\Delta\nu/\Delta$ASA		0.7	10.8	13.11	24.7

[a] All values were obtained from the simulations assuming $R = 1.0$ nm in eq 1. The preferential binding has been decomposed into contributions from anions and cations ($\nu = \nu^+ + \nu^-$) assuming that $\nu^+ = N_{s+} - (\rho_+/\rho_w)\, N_{sw}$, etc. Changes in accessible surface area (ΔASA) are taken from Table 5.

2.6±1.1, indicating an overall stabilization of the unfolded state over the folded state. The pmf calculation determined the fraction of folded peptide to be 0.53±0.03 in pure water. Using this ratio, the value of ν_{sc}, and the KB data from Table 6 in Equation 7, leads to a predicted folded population of 0.21±0.09 in 2 M salt solution. This is in reasonable agreement with the ratio of 0.12±0.05 determined from the pmf calculation in saline solution. The small discrepancy was probably due to the presence of multiple unfolded conformations that would not have been sampled with their correct Boltzmann weights, and the use of only one simulated salt concentration to characterize the entire salt effect. However, the results demonstrate that a combination of simulation data and KB theory can be used to provide quantitative information concerning the effects of cosolvents on conformational equilibria in biological systems. They also highlight the need to investigate changes in the cosolvent distribution around biomolecules extending over several solvation shells.

An attempt was also made to decompose the preferential binding into contributions from sodium and chloride ions, and from the different residues or groups present in the peptide. The anion and cation contributions are also presented in Tables 7 and 8. The effect of the anions and cations on LE was very similar, corresponding to approximately half the total preferential interaction. This could have been the result of local electroneutrality constraints, or due to the large self-association of the ions in solution, as indicated by the positive G_{cc} value of 286 cm^3/mol (see Table 6).

Tanford has suggested that the total free energy, and hence the corresponding preferential interactions, for transferring proteins from water to a cosolvent solution can be decomposed into a sum of group effects.[50] A similar decomposition was attempted here by assigning each ion and water surrounding

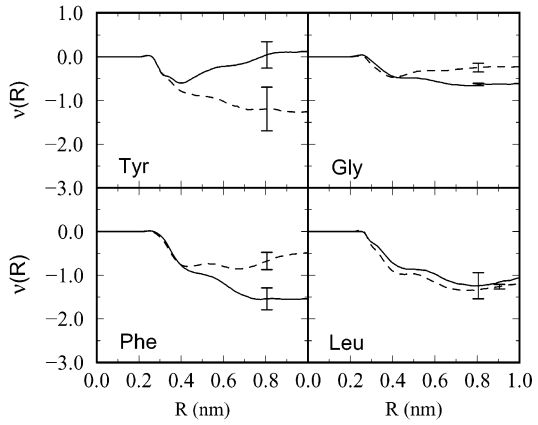

Figure 6. Residue-based cosolvent preferential binding parameters (eqs 1 and 5) for the folded (solid line) and the unfolded (dashed line) conformations as a function of integration distance *R*.

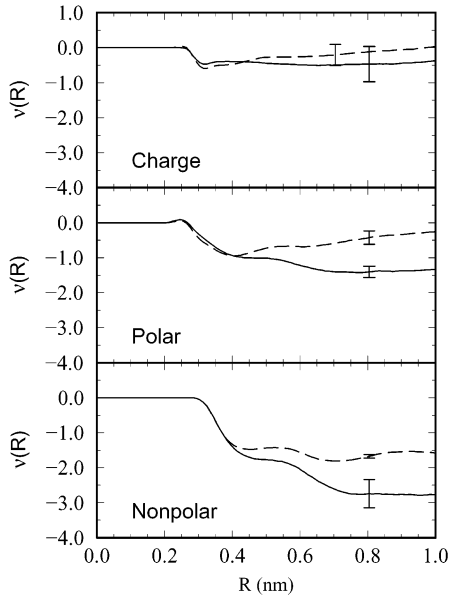

Figure 7. Group-based cosolvent preferential binding parameters (eqs 1 and 5) between the folded (solid line) and unfolded (dashed line) conformations as a function of integration distance *R*.

the peptide to the preferential interaction for the group to which the ion or water was the closest. The first decomposition was into residues with both glycines being included together. The results are displayed in Figure 6 and included in Table 7. The plots of $\nu_{sc}(R)$ displayed reasonable plateau values at 1.0 nm, indicating the salt and water distributions had reached their bulk values. The data suggested that the major contributions were from the Tyr and Phe residues with smaller contributions from Gly and Leu. Alternatively, the decomposition into charged, polar and hydrophobic groups displayed in Figure 7 suggested that the polar and hydrophobic groups contributed the largest effect. However, the change in preferential binding per unit change in solvent accessible surface area indicated an increased preferential binding of salt on exposure of hydrophobic surface area. This is opposite to the experimentally observed salting-out effect on small hydrophobic solutes,[7,29,41] and previous studies using similar force fields,[51] which all suggest a decrease in preferential interaction with NaCl on increasing the hydrophobic surface area. Hence, it appears that a simple meaningful decomposition is difficult to obtain for LE.

There are several possible reasons for this. First, a simple decomposition may not be possible due to the importance of cooperative effects. Alternatively, the decomposition for a small peptide such as LE may be complicated by the irregular shape of the peptide. It is possible that the presumed preferential interaction with the exposed charged groups was assigned to the Tyr, Phe and hydrophobic groups because they present a much larger surface area. Hence, the ions may have been assigned to these groups even though they were really attracted to the charged termini. A protein, with a surface of less curvature, may prove easier to assign individual ion and water molecules to specific groups. Clearly, more effort is required to determine the feasibility of performing such decompositions.

In many cases one would like to determine changes in cosolvent association (ΔN_{sc}) with the peptide rather than changes in preferential binding ($\Delta\nu_{sc}$). Cosolvent association is only one component of the preferential binding, water association being the other. Here we demonstrate that, under certain circumstances, it is possible to use KB theory to obtain information concerning cosolvent changes alone. The KB result for the partial molar volume (pmv) of an infinitely dilute solute ($\bar{V}_s^{\infty}$) in a binary solvent mixture is given by[24]

$$\bar{V}_s^{\infty} = RT\kappa_T - \phi_c G_{sc} - \phi_w G_{sw} \tag{8}$$

where κ_T is the isothermal compressibility of the cosolvent solution, $\phi_i = \rho_i \bar{V}_i$ is the volume fraction of the species *i* in solution, and $\bar{V}_i$ is the partial molar volume of *i*. If one considers the change in partial molar volumes between the folded and unfolded states ($\Delta\bar{V}_s^{\infty}$) one can write

$$\Delta N_{sw}\bar{V}_w + \Delta N_{sc}\bar{V}_c + \Delta\bar{V}_s^{\infty} = 0 \tag{9}$$

Here, ΔN_{sc} and ΔN_{sw} are the change in cosolvent and water association on going from the folded to the unfolded state. This simply states that the total volume of the system does not change due to a change in conformation of an infinitely dilute solute. The above expression can be rearranged to give

$$\Delta N_{sc} = \phi_w \Delta\nu_{sc} - \rho_c \Delta\bar{V}_s^{\infty} \tag{10}$$

where we now show that the last term is negligible.

The peptide pmv can be obtained from the volume of the simulated system as a function of the conformation of the peptide. Subtracting the volume of the solvent mixture (obtained from simulations in the absence of the peptide) provides the required pmv of the peptide. Using this approach the partial molar volumes of the folded and unfolded forms of LE were determined to be 379 and 367 cm^3/mol, respectively, in pure water compared to 434 and 410 cm^3/mol, respectively, in saline solution. Consequently, the corresponding changes in partial molar volume on unfolding were −12 and −24 cm^3/mol for pure water and saline solution, respectively. The data clearly illustrated that the change in the peptide pmv accompanying a change from the folded to the unfolded state was small, on the order of the volume of one water molecule (18 cm^3/mol), and in agreement with other estimates for similar systems.[52,53] Hence, the value of $\rho_c\Delta\bar{V}_s^{\infty}$ was approximately 0.1 for 2 M NaCl, which is small (4%) compared to the first term on the rhs of eq 10 where $\Delta\nu_{sc} = 2.6\pm1.1$ and $\phi_w = 0.95$. Consequently, for situations where the change in solute volume is small, the difference in cosolvent association (ΔN_{sc}) can be obtained from the change in preferential binding ($\Delta\nu_{sc}$) by reference to the properties of the cosolvent solution (ϕ_w). This provides a thermodynamic relationship between changes in preferential binding, which is valid for a number of models, and the change in cosolvent association, which is generally more difficult to

isolate.[13,14] From the simulations described here the change in cosolvent association was 2.5, i.e. slightly more than the ion pair required to neutralize both terminal groups.

Conclusions

The system studied here represents a simple model of an equilibrium process in solution which is affected by the addition of salt. A consistent description of the change in the equilibrium was obtained using both pmf calculations and a combination of MD and KB theory. It was not the purpose of this study to directly compare with experimental data. In fact, the simulated properties of the saline solution suggest that the agreement with experiment may be poor. However, the results indicate that it is feasible to use a combination of MD and KB theory to quantitatively study cosolvent effects on peptides and proteins. This is especially important for systems containing larger peptides or proteins where one cannot use the pmf approach to determine changes in conformational populations.

The present calculations were computationally intensive as the ion distribution changes slowly. This was, at least in part, due to the low ratio of ions to water molecules present in the current simulations, together with the relatively weak interaction that the ions have with the peptide. Applying the same techniques to studies of urea or guanidinium chloride denaturation, or secondary structure induction by fluorinated alcohols or ketones, where the effects are larger and involve higher cosolvent concentrations, should provide significant increases in precision. The linear approximation used in the generation of eq 7 is expected to be good for the study of salt, urea, and guanidinium chloride effects. However, TFE effects may require the determination of the preferential binding at multiple cosolvent concentrations before the appropriate integration can be performed.

The effect of salt on the equilibrium was to favor more extended structures possessing an exposed carboxylate terminus. This result is consistent with a simple charge screening effect leading to destabilization of the folded state, or stabilization of the unfolded state. Very little direct binding to the peptide was observed. Decomposition of the preferential binding into anion and cation components produced reasonable results. However, one should always remember that the effects of the anions and cations are coupled, due to the specific interactions between anions and cations, and hence it is not possible to obtain an intrinsic sodium or chloride ion effect.[54] Decomposition of the preferential binding into peptide residues or groups did not produce sensible results.

Acknowledgment. This project was supported by the NSF and the ACS Petroleum Research Fund.

References and Notes

(1) Privalov, P. L. *Crit. Rev. Biochem. Mol. Biol.* **1990**, *25*, 281−305.
(2) Makhatadze, G. I.; Privalov, P. L. *J. Mol. Biol.* **1993**, *232*, 639−659.
(3) Zipp, A.; Kauzmann, W. *Biochemistry* **1973**, *12*, 4217−4228.
(4) Arakawa, T.; Timasheff, S. N. *Biochemistry* **1987**, *26*, 5147−5153.
(5) Timasheff, S. N. *Adv. Prot. Chem.* **1998**, *51*, 355−433.
(6) Santoro, M. M.; Liu, Y.; Khan, S. M.; Hou, L.; Bolen, D. W. *Biochemistry* **1992**, *31*, 5278−5283.
(7) von Hippel, P. H.; Schleich, T. *Acc. Chem. Res.* **1969**, *2*, 257−265.
(8) Collins, K. D.; Washabaugh, M. L. *Q. Rev. Biochem.* **1985**, *18*, 323−422.
(9) Arakawa, T.; Timasheff, S. N. *Biochemistry* **1982**, *21*, 6545−6552.
(10) Buck, M. *Q. Rev. Biophys.* **1998**, *31*, 297−355.
(11) Arakawa, T.; Timasheff, S. N. *Biochemistry* **1984**, *23*, 5912−5923.
(12) Arakawa, T.; Timasheff, S. N. *Biochemistry* **1984**, *23*, 5924−5929.
(13) Makhatadze, G. I.; Privalov, P. L. *J. Mol. Biol.* **1992**, *226*, 491−505.
(14) Schellman, J. A.; Gassner, N. C. *Biophys. Chem.* **1996**, *59*, 259−275.
(15) Schellman, J. A. *Biopolymers* **1994**, *34*, 1015−1026.
(16) Smith, P. E.; Pettitt, B. M. *J. Am. Chem. Soc.* **1991**, *113*, 6029−6037.
(17) Smith, P. E.; Marlow, G. E.; Pettitt, B. M. *J. Am. Chem. Soc.* **1993**, *115*, 7493−7498.
(18) Marlow, G. E.; Pettitt, B. M. *Biopolymers* **2001**, *60*, 134−152.
(19) Roccatano, D.; Colombo, G.; Fiorono, M.; Mark, A. E. *Proc. Natl. Acad. Sci. U.S.A.* **2002**, *99*, 12179−12184.
(20) Tirado-Rives, J.; Orozco, M.; Jorgensen, W. L. *Biochemistry* **1997**, *36*, 7313−7329.
(21) Caflisch, A.; Karplus, M. *Struct. Fold. Des.* **1999**, *7*, 477−488.
(22) Marlow, G. E.; Pettitt, B. M. *Biopolymers* **2003**, *68*, 192−209.
(23) Kirkwood, J. G.; Buff, F. P. *J. Chem. Phys.* **1951**, *19*, 774−777.
(24) Ben-Naim, A. *Statistical Thermodynamics for Chemists and Biochemists.*; Plenum Press: New York, 1992.
(25) Hughes, J.; Smith, T. W.; Kosteriltz, H. W.; Fothergill, L. A.; Morgan, B. A.; Morris, H. R. *Nature* **1975**, *258*, 577−579.
(26) Aburi, M.; Smith, P. E. *Biopolymers* **2002**, *64*, 177−188.
(27) Nandi, P. K.; Robinson, R. D. *J. Am. Chem. Soc.* **1972**, *94*, 1299−1308.
(28) Nandi, P. K.; Robinson, R. D. *J. Am. Chem. Soc.* **1972**, *94*, 1308−1315.
(29) Clever, H. L.; Young, C. L. *IUPAC Solubility data series*; Pergamon Press: Oxford, 1987; Vol. 27/28 (Methane).
(30) Scott, W.; Hunenberger, P. H.; Tironi, I. G.; Mark, A. E.; Billeter, S. R.; Fennen, J.; Torda, A. E.; Huber, T.; Kruger, P.; van Gunsteren, W. F. *J. Phys. Chem. A* **1999**, *103*, 3596−3607.
(31) Berendsen, H. J. C.; Postma, J. P.; van Gunsteren, W. F.; Hermans, J. Interaction models for water in relation to protein hydration in *Intermolecular forces*; Pullman, B., Ed.; D. Reidel: Dordrecht, 1981; pp 331−342.
(32) Ryckaert, J. P.; Ciccotti, G.; Berendsen, H. J. C. *J. Comput. Phys.* **1977**, *23*, 327−341.
(33) Tironi, I. G.; Sperb, R.; Smith, P. E.; van Gunsteren, W. F. *J. Chem. Phys.* **1995**, *102*, 5451−5459.
(34) Smith, P. E.; van Gunsteren, W. F. *J. Chem. Phys.* **1994**, *100*, 3169−3174.
(35) van Gunsteren, W. F.; Berendsen, H. J. C. *Angew. Chem., Int. Ed. Engl.* **1990**, *29*, 992−1023.
(36) Allen, M. P.; Tildesley, D. J. *Computer Simulation of Liquids*; Clarendon Press: Oxford, 1987.
(37) Kumar, S.; Bouzida, D.; Swendsen, R. H.; Kollman, P.; Rosenberg, J. M. *J. Comput. Chem.* **1992**, *13*, 1011−1021.
(38) Karpen, M. E.; Tobias, D. J.; Brooks, C. L., III. *Biochemistry* **1993**, *32*, 412−420.
(39) Daura, X.; Antes, I.; van Gunsteren, W. F.; Thiel, W.; Mark, A. E. *Proteins* **1999**, *36*, 542−555.
(40) Matteoli, E.; Mansoori, G. A. In *Advances in thermodynamics; Fluctuation Theory of Mixtures*; Taylor & Francis; New York, 1990.
(41) Schumpe, A. *Chem. Eng. Sci.* **1993**, *48*, 153−158.
(42) Friedman, H.; Ramanathan, P. S. *J. Phys. Chem.* **1970**, *74*, 3756−3765.
(43) Kusalik, P. G.; Patey, G. N. *J. Chem. Phys.* **1987**, *86*, 5110−5116.
(44) Behera, R. *J. Chem. Phys.* **1998**, *108*, 3373−3374.
(45) Rajappa, C.; Smith, P. E. *J. Phys. Chem. B* **2002**, *106*, 1491−1500.
(46) Rajappa, C.; Smith, P. E. *J. Chem. Phys.* **2001**, *114*, 426−435.
(47) Rajappa, C.; Smith, P. E. *J. Chem. Phys.* **2001**, *115*, 5521−5530.
(48) Rajappa, C.; Smith, P. E. *J. Phys. Chem. B* **2002**, *105*, 11513−11522.
(49) Weerasinghe, S.; Smith, P. E. *J. Chem. Phys.* **2003**, *118*, 5901−5910.
(50) Tanford, C. *Adv. Prot. Chem.* **1970**, *24*, 1−95.
(51) Smith, P. E. *J. Chem. Phys.* **1999**, *111*, 5568−5579.
(52) Imai, T.; Harano, Y.; Kovalenko, A.; Hirata, F. *Biopolymers* **2001**, *59*, 512−519.
(53) Royer, C. A. *Biochim. Biophys. Acta* **2002**, *1595*, 201−209.
(54) Perkyns, J. S.; Pettitt, B. M. *Biophys. Chem.* **1994**, *51*, 129−146.
(55) Lee, B.; Richards, F. M. *J. Mol. Biol.* **1971**, *55*, 379−400.